

## Dynamic Approach to the Fully Frustrated XY Model

H. J. Luo,<sup>1</sup> L. Schülke,<sup>1</sup> and B. Zheng<sup>2</sup>

<sup>1</sup>Universität-GH Siegen, D-57068 Siegen, Germany

<sup>2</sup>Universität Halle, D-06099 Halle, Germany

(Received 26 January 1998)

Using Monte Carlo simulations, we systematically investigate the nonequilibrium dynamics of the chiral degree of freedom in the two-dimensional fully frustrated XY model. By means of the short-time dynamics approach, we estimate the second order phase transition temperature  $T_c$  and all the dynamic and static critical exponents  $\theta$ ,  $z$ ,  $\beta$ , and  $\nu$ . [S0031-9007(98)06479-5]

PACS numbers: 75.10.Hk, 64.60.Cn, 64.60.Ht, 75.40.Mg

For critical phenomena, it is traditionally believed that universal behavior exists only in equilibrium or in the long-time regime of the dynamical evolution. The universal scaling behavior is described by a number of critical exponents. Because of critical slowing down, numerical measurements of the critical exponents are very difficult.

Recently, much progress has been achieved in dynamic critical phenomena. It was discovered that, already after a microscopic time scale  $t_{\text{mic}}$ , universal scaling behavior emerges in the *macroscopic short-time regime* of the dynamic process [1–6]. We first consider the following dynamic relaxation process: a magnetic system initially in a high-temperature state with a small initial magnetization  $m_0$  is quenched to the critical temperature  $T_c$  without an external magnetic field and then released to dynamic evolution of model A. The dynamics of model A is a relaxational dynamics without conservation of energy and order parameter [7]. At the onset of the evolution, the magnetization is subjected to the scaling form [1,4,5,8,9]

$$M(t, \tau, m_0) \sim m_0 t^\theta F(t^{1/\nu z} \tau). \quad (1)$$

The exponent  $\theta$  is a new independent exponent,  $\tau \sim (T - T_c)/T_c$  is the reduced temperature,  $\beta$  and  $\nu$  are the static critical exponents, and  $z$  is the dynamic exponent. At the critical temperature,  $\tau = 0$ , the magnetization undergoes a *critical initial increase*  $M(t) \sim t^\theta$ .

Another important example is the dynamic relaxation of a magnetic system starting from an ordered state ( $m_0 = 1$ ) [6,9–11]. The scaling form of the  $k$ th moment of the magnetization for this dynamic process is given by

$$M^{(k)}(t, \tau, L) = b^{-k\beta/\nu} M^{(k)}(b^{-z} t, b^{1/\nu} \tau, b^{-1} L), \quad (2)$$

where, for later convenience, a system with finite size  $L$  has been considered.

One prominent property of the scaling forms (1) and (2) is that the exponents  $\beta$ ,  $\nu$ , and  $z$  take the same values as in equilibrium or in the long-time regime of the dynamic evolution. It has been suggested that it is possible to determine not only the dynamic but also all the *static* exponents as well as the *critical temperature* already in the short-time regime [5,9] (see also Refs. [6,11–13]). The method may be an alternative way for overcoming critical slowing down since the

measurement does not enter the long-time regime. It is important to systematically verify this application in general and complex models.

The two-dimensional fully frustrated XY (FFXY) model has been the topic of many recent studies [14–21]. Critical properties of this model are rather unconventional. On the square lattice, the model has two kinds of phase transitions, i.e., the Kosterlitz-Thouless phase transition (XY-like) and the second order phase transition (Ising-like). Numerical simulations of the FFX model suffer severely from critical slowing down. Because of the frustration, the standard cluster algorithm does not apply to the FFX model. Most of the recent work on FFX models supports that these two phase transitions take place at two different temperatures; however, their critical properties are still not very clear. For example, for the second order phase transition the estimated values of the exponents  $\beta$  and  $\nu$  differ in the literature [16,17,20,21] and the critical dynamics has not been investigated. It is still a matter of controversy whether the chiral degree of freedom of the FFX model is in the same universality class as the Ising model [20–23].

In this Letter we present results of systematic Monte Carlo simulations for the short-time dynamic behavior of the second order phase transition in the two-dimensional FFX model. For the first time, we determine the dynamic exponents  $\theta$  and  $z$ . Based on the short-time dynamic scaling, the static exponents  $\beta$  and  $\nu$  as well as the critical temperature  $T_c$  are also extracted from the numerical data.

The Hamiltonian of the FFX model on a square lattice can be written as

$$H = -K \sum_{\langle ij \rangle} f_{ij} \cos(\theta_i - \theta_j), \quad (3)$$

In our notation  $K$  is simply the inverse temperature,  $\theta_i$  is the angle of the spin (a unit vector) located on site  $i$ ,  $f_{ij}$  determine the frustration, and the sum is over the nearest neighbors. A simple realization of the FFX model is by taking  $f_{ij} = -1$  on half of the vertical links and  $f_{ij} = 1$  on other links, e.g., as shown in Fig. 1. The order parameter for the second order phase transition is the staggered chiral magnetization defined as [18]

$$M_I = \left\langle \frac{1}{L^2} \sum_r (-1)^{r_x+r_y} \operatorname{sgn} \sum_{(ij) \in P_r} f_{ij} \sin(\theta_i - \theta_j) \right\rangle, \quad (4)$$

where  $(r_x, r_y)$  is the coordinate of the plaquette  $P_r$ .

At first, we investigate the short-time critical behavior of  $M_I$  in the dynamic process starting from an initial state with a very high temperature and a small magnetization  $m_0$ . To prepare an initial configuration, first we randomly generate all spins on the lattice, then randomly choose a number of plaquettes and orient their spins according to the configuration of the ground state as shown in Fig. 1 until the initial magnetization  $m_0$  is achieved. After the initial configuration is generated, the system is released to the dynamic evolution with the Metropolis algorithm at temperatures around  $T_c$ . We have performed our simulation on lattices of size  $L = 128$  and 256. The average is taken over independent initial configurations with 40 000 samples for  $L = 128$  and 10 000 samples for  $L = 256$ . Errors are estimated by dividing the samples into three groups.

In order to locate the critical temperature  $T_c$ , simulations have been carried out with three temperatures  $T = 0.452, 0.454, \text{ and } 0.456$ . The initial magnetization is set to  $m_0 = 0.06$ . In Fig. 2, the time evolution of the magnetization  $M_I(t)$  at different temperatures is plotted with solid lines in log-log scale for the lattice size  $L = 128$ . Data within the microscopic time scale  $t_{\text{mic}} \sim 100$ , which are dependent on microscopic details, are not included. Indeed we observe that the magnetization increases at the macroscopic early time. The magnetization at the temperature between  $T = 0.452$  and 0.456 can be obtained by quadratic interpolation. From the scaling form (1) and as suggested in Ref. [9], searching for a curve  $M_I(t)$  with the best power law behavior can yield an estimate of the critical temperature. In Fig. 2, the dotted line represents such a curve and the corresponding critical temperature

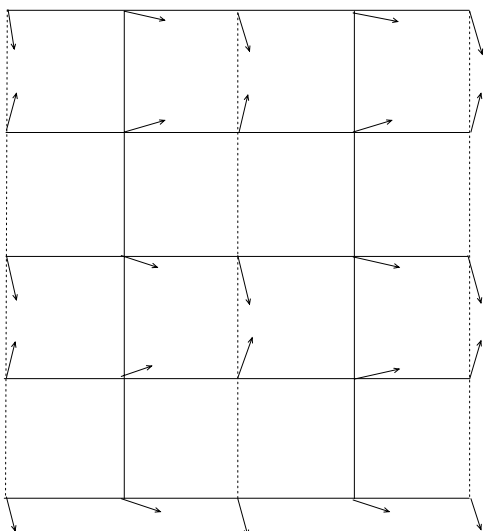


FIG. 1. One of the ground states of the FFX model.

$T_c = 0.4547(8)$ . From the slope of this curve, the exponent  $\theta = 0.200(3)$  is obtained.

From an analysis of the data for  $L = 256$  and also for  $m_0 = 0.04$  we have observed that the finite size effect for  $L = 128$  and the finite  $m_0$  effect for  $m_0 = 0.06$  are already sufficiently small to be neglected. The fact that the finite size effect can easily be controlled in the short-time dynamics is an advantage of the short-time dynamic approach.

In principle, with  $T_c$  in hand other static and dynamic critical exponents can now be obtained. For example,  $1/\nu z = 0.59(3)$  is estimated from  $\partial_\tau \ln M_I(t, \tau)|_{\tau=0}$ . However, our data show that to determine these exponents or the critical temperature  $T_c$ , a dynamic process starting from an ordered state is preferable, since the fluctuation is weaker.

For this purpose, simulations were also performed with temperatures  $T = 0.452, 0.454, \text{ and } 0.456$ , starting from an ordered initial state. The lattice size chosen was  $L = 256$  and the system was updated for 2000 Monte Carlo steps. The average was taken over 2000 samples. The ordered initial state was taken to be the ground state shown in Fig. 1.

The estimation of  $T_c$  can now be performed again. From the scaling form (2) and for sufficiently large  $L$  we can easily deduce the scaling behavior for the magnetization ( $k = 1$ )

$$M_I(t, \tau) = t^{-\beta/\nu z} G(t^{1/\nu z} \tau). \quad (5)$$

As pointed out earlier, the temperature for which the magnetization has the best power law behavior is the critical temperature  $T_c$ . In Fig. 3, the time evolution of  $M_I(t)$  at  $T = 0.452, 0.454, \text{ and } 0.456$  is plotted in log-log scale.  $M_I(t)$  at other temperatures in the interval  $[0.452, 0.456]$  can be estimated by a quadratic interpolation. The

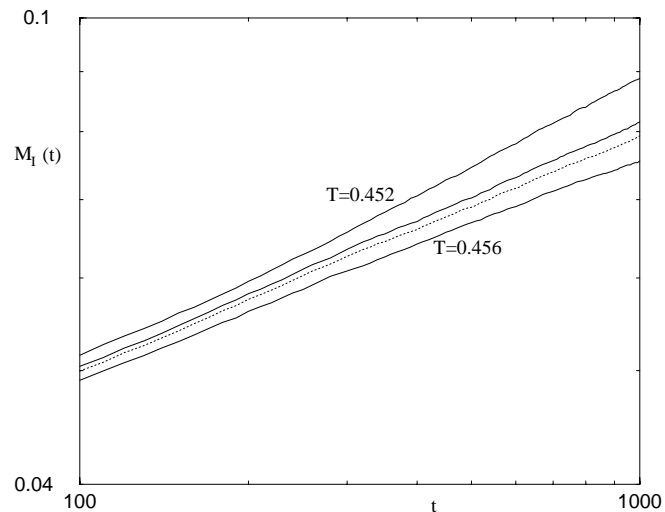


FIG. 2. The chiral magnetization  $M_I(t)$  starting from a disordered state. The temperatures for solid lines are  $T = 0.452, 0.454$  and 0.456 from above. The dotted line represents  $M_I(t)$  at  $T_c = 0.4547$ .

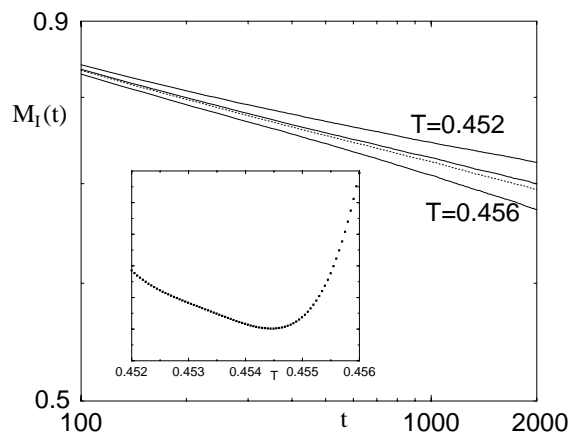


FIG. 3. The chiral magnetizations  $M_I(t)$  starting from an ordered state. From above, the solid lines represent  $M_I(t)$  at  $T = 0.452, 0.454,$  and  $0.456$ . The dotted line is at  $T_c = 0.4545$ . The inset displays the deviation of  $M_I(t)$  from the power law behavior.

deviation from the power law can be estimated in different ways. In this paper, we measure the deviation as the error by fitting  $M_I(t)$  directly to a power law in the time interval  $[200, 2000]$ . Furthermore, we perform the fitting in log scale, i.e., less weight is given to the data in the longer time regime. In the inset of Fig. 3, the deviation of  $M_I$  from the power law is plotted as a function of the temperature. The clear minimum confidently indicates the critical temperature  $T_c$ . The resulting value  $T_c = 0.4545(2)$  is consistent with  $T_c = 0.4547(8)$  obtained from Fig. 2 and very close to those values ranging from  $T_c = 0.451$  to  $0.454$  reported in most of the recent references [16,17,20,21]. Our statistical error, however, is smaller. The corresponding magnetization is also plotted in Fig. 3 with a dotted line. The slope of this curve yields the critical exponent  $\beta/\nu z = 0.0602(2)$ . The quality of this measurement is very good. With  $\beta/\nu$  given, one can obtain a rigorous  $z$  or vice versa [6,9–11,25]. As compared to simulations with a disordered initial state, the measurements here carry considerably fewer fluctuations.

To extract the critical exponent  $1/\nu z$ , differentiation of Eq. (5) leads to

$$\partial_\tau \ln M_I(t, \tau)|_{\tau=0} = t^{1/\nu z} \partial_{\tau'} \ln G(\tau')|_{\tau'=0}. \quad (6)$$

Therefore,  $\partial_\tau \ln M_I(t, \tau)|_{\tau=0}$  should also present a power law behavior in the beginning of the time evolution. In Fig. 4(a),  $\partial_\tau \ln M_I(t, \tau)$  at  $T_c = 0.4545$  is plotted in log-log scale. The power law behavior is clearly seen. The slope yields the critical exponent  $1/\nu z = 0.57(1)$ .

The final step is to seek the dynamical critical exponent  $z$ . For this, we introduce a time-dependent Binder cumulant  $U(t, L) = M_I^{(2)}/M_I^2 - 1$ . Because of the short spatial correlation length in the short-time regime, a simple finite size scaling analysis shows at the critical temperature

$$U(t, L) \sim t^{d/z}. \quad (7)$$

In Fig. 4(b), the curve for  $U(t, L)$  in log-log scale shows a nice power law behavior. The slope gives the critical

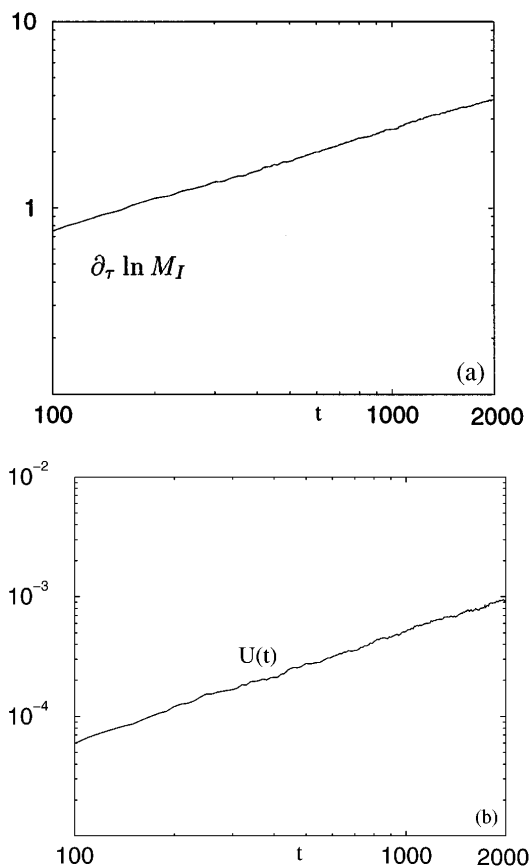


FIG. 4. (a) The derivative  $\partial_\tau \ln M_I(t, \tau)|_{\tau=0}$  plotted versus time in log-log scale. (b) The Binder cumulant  $U$ .

exponent  $d/z = 0.92(2)$ . Table I summarizes the results. The errors in the measurements from  $m_0 = 1$  are clearly smaller than those from  $m_0 = 0.06$ .

From the Binder cumulant one can estimate independently the dynamic exponent  $z$ . With  $z$  in hand, we calculate the critical exponents  $2\beta/\nu$  and  $\nu$  from  $\beta/\nu z$  and  $1/\nu z$ . Table II lists all critical exponents along with the results reported in the recent literature. Now  $\theta = 0.202(3)$  is measured at  $T_c = 0.4545$ , which shows a small difference from that at  $T = 0.4547$ . Our short-time dynamic measurements support those from Ref. [17] and provide extra new results for the dynamic exponents  $z$  and  $\theta$ . The exponent  $\nu$  of the FFX model is different from that of the Ising model by nearly 20%. This indicates that the chiral degree of freedom of the FFX model is in a new universality class. Other exponents of the FFX model do not differ much from those of the Ising model. From our numerical data, we observe that the values of the critical exponents are sensitive to the assumed or measured

TABLE I. The critical temperature and the critical exponents from dynamic measurements.

$m_0$	$T_c$	$\theta$	$\beta/\nu z$	$1/\nu z$	$d/z$
1	0.4545(2)		0.0602(2)	0.57(1)	0.92(2)
0.06	0.4547(8)	0.200(3)		0.59(3)	

TABLE II. Critical exponents obtained in this work and values reported in some recent references. Reference [20] does not provide an estimate of the error on  $\nu = 1$ . For the Ising model, exponents  $\nu$  and  $2\beta/\nu$  are exact values and  $\theta$  is taken from Refs. [8,27]. The exponent  $z$  in the literature ranges from 2.155 to 2.172 [6,8,25,27]. Here an “average” value is given.

	This work	Ref. [21] (1996)	Ref. [20] (1995)	Ref. [17] (1994)	Ref. [16] (1993)	Ising
$T_c$	0.4545(2)	0.451(1)	0.452(1)	0.454(2)	0.454(3)	
$\nu$	0.81(2)	0.898(3)	1	0.813(5)	0.80(5)	1
$2\beta/\nu$	0.261(5)			0.22(2)	0.38(2)	0.25
$z$	2.17(4)					2.165(10)
$\theta$	0.202(3)					0.191(3)

critical temperature  $T_c$ . This should be a main reason for the different values of the exponents reported in the literature. Figure 2 and, in particular, Fig. 3, give us confidence in our measurements of the critical temperature  $T_c$ . Furthermore, our exponent  $\nu$  is extracted from the data in the close neighborhood of  $T_c$ , in contrast to many simulations in equilibrium. The finite size effect is also well under control in the short-time dynamic approach.

In conclusion, using Monte Carlo methods, we have systematically investigated and confirmed the universal short-time dynamic behavior of the second order phase transition in the two-dimensional FFX model. Based on the short-time dynamic scaling form, all static and dynamical critical exponents are determined. The exponents  $\theta$  and  $z$  are obtained for the first time and the measurement of the exponent  $\beta/\nu z$  and the critical temperature  $T_c$  is very precise. The estimated value  $\nu = 0.81(2)$  is clearly different from  $\nu = 1$  for the Ising model. Our investigation of the chiral degree of freedom of the FFX model is to date the most systematic. We are convinced that the short-time dynamic approach is not only conceptually interesting but also practically efficient. In the simulations we do not encounter difficulties associated with large correlation times since our measurements are carried out in the short-time regime, and we do not have the problem of generating independent configurations.

A possible extension of the present work is the Kosterlitz-Thouless phase transition [24,26]. However, owing to the absence of symmetry breaking, a clear signal such as in Fig. 3 does not exist for the Kosterlitz-Thouless transition temperature  $T_{KT}$ . The determination of  $T_{KT}$  and of the exponent  $\nu$  is very difficult and requires extensive simulations and a careful analysis.

Work supported in part by the Deutsche Forschungsgemeinschaft; Schu 95/9-1 and SFB 418.

[1] H.K. Janssen, B. Schaub, and B. Schmittmann, Z. Phys. B **73**, 539 (1989).

- [2] D. A. Huse, Phys. Rev. B **40**, 304 (1989).  
 [3] K. Humayun and A.J. Bray, J. Phys. A **24**, 1915 (1991).  
 [4] Z. B. Li, U. Ritschel, and B. Zheng, J. Phys. A **27**, L837 (1994).  
 [5] L. Schülke and B. Zheng, Phys. Lett. A **204**, 295 (1995).  
 [6] B. Zheng, “Monte Carlo Simulations of Short-Time Critical Dynamics” (to be published).  
 [7] P. C. Hohenberg and B. I. Halperin, Rev. Mod. Phys. **49**, 435 (1977).  
 [8] P. Grassberger, Physica (Amsterdam) **214A**, 547 (1995).  
 [9] L. Schülke and B. Zheng, Phys. Lett. A **215**, 81 (1996).  
 [10] D. Stauffer, Physica (Amsterdam) **186A**, 197 (1992).  
 [11] D. Stauffer and R. Knecht, Int. J. Mod. Phys. **C7**, 893 (1996).  
 [12] Z. B. Li, L. Schülke, and B. Zheng, Phys. Rev. E **53**, 2940 (1996).  
 [13] R. E. Blundell, K. Humayun, and A. J. Bray, J. Phys. A **25**, L733 (1992).  
 [14] J. Lee, J. M. Kosterlitz, and E. Granato, Phys. Rev. B **43**, 11 531 (1991).  
 [15] G. Ramirez-Santiago and J. José, Phys. Rev. Lett. **68**, 1224 (1992).  
 [16] E. Granato and M. P. Nightingal, Phys. Rev. B **48**, 7438 (1993).  
 [17] S. Lee and K. Lee, Phys. Rev. B **49**, 15 184 (1994).  
 [18] G. Ramirez-Santiago and J. V. José, Phys. Rev. B **49**, 9567 (1994).  
 [19] S. J. Lee, J. R. Lee, and B. Kim, Phys. Rev. E **51**, R4 (1995).  
 [20] P. Olsson, Phys. Rev. Lett. **75**, 2758 (1995).  
 [21] J. V. José and G. Ramirez-Santiago, Phys. Rev. Lett. **77**, 4849 (1996).  
 [22] P. Olsson, Phys. Rev. Lett. **77**, 4850 (1996).  
 [23] P. Olsson, Phys. Rev. B **55**, 3585 (1997).  
 [24] H. J. Luo, L. Schülke, and B. Zheng, Phys. Rev. E **57**, 1327 (1998).  
 [25] N. Ito, Physica (Amsterdam) **196A**, 591 (1993).  
 [26] H. J. Luo and B. Zheng, Mod. Phys. Lett. B **11**, 615 (1997).  
 [27] K. Okano, L. Schülke, K. Yamagishi, and B. Zheng, Nucl. Phys. **B485**, 727 (1997).